

Calculated solar-neutrino capture rate for a radiochemical ^{205}Tl -based solar-neutrino detector

Joel Kostensalo* and Jouni Suhonen†
Department of Physics, University of Jyväskylä, Finland

K. Zuber‡
Institute for Nuclear and Particle Physics, TU Dresden, 01069 Dresden, Germany
(Dated: December 12, 2019)

Radiochemical experiments for low-energy solar-neutrino detection have been making headlines by exploiting the isotopes ^{37}Cl and ^{71}Ga . Such a very low-threshold measurement of this type can also be performed using ^{205}Tl , which has been considered for decades for this purpose. A unique feature of this detector nucleus is the integration is the solar-neutrino flux over millions of years owing to its long-living daughter ^{205}Pb . In this study we have calculated for the first time the cross section for the charged-current solar-neutrino scattering off ^{205}Tl . Taking into account the solar-model-predicted neutrino fluxes and the electron-neutrino survival probabilities, a solar-neutrino capture rate of 62.2 ± 8.6 SNU is determined, a value significantly smaller than in previous estimates.

I. INTRODUCTION

Neutrinos play a key role in several aspects of astroparticle and nuclear physics [1]. From the astrophysical point of view solar neutrinos can be monitored in real-time measurements which allows to study neutrino properties and also stellar structure and evolution. To date real-time monitoring of various neutrino chain reactions has been done by the Super-Kamiokande, the Sudbury Neutrino Observatory (SNO), KamLAND, and especially Borexino. Borexino was able to perform a common global fit of all the observed reactions of pp, pep, ^7Be and ^8B in one detector [2].

An alternative method to the above-mentioned ones, used by the first solar-neutrino experiments, are the radio-chemical observations. These experiments employ the charged-current neutrino-nucleus scattering reaction

$$\nu_e + (A, Z) \rightarrow e^- + (A, Z + 1) \quad (1)$$

for solar-neutrino detection. This reaction has been used in the pioneering Homestake experiment using ^{37}Cl as detector material [3] and in this experiment a deficit with respect to expectation was found. First measurements of the fundamental pp-neutrinos were based on ^{71}Ga (GALLEX, GNO, SAGE). Several other nuclides, with different reaction thresholds, have been considered for more refined overall spectral analyses [4]. A very interesting candidate of this type is ^{205}Tl , which has a very low threshold for solar neutrinos.

II. THE ^{205}Tl REACTION

The dominant charged-current neutrino-nucleus reaction under discussion is

$$^{205}\text{Tl}(1/2^+) + \nu_e \rightarrow ^{205}\text{Pb}(1/2^-) + e^-, \quad (2)$$

which feeds the first excited state of ^{205}Pb at 2.33 keV and is of first-forbidden non-unique type [5]. Only a tiny portion of the feeding goes to the $5/2^-$ ground state of ^{205}Pb , the corresponding transition being first-forbidden unique [5, 6]. According to the current Atomic Mass Evaluation [7] the Q -value is given by 50.6 ± 0.5 keV, which is so far the lowest threshold among radiochemical approaches for solar-neutrino detection. This results in a total threshold of about 53 keV for the transition (2). Furthermore, a unique feature of this reaction is the possibility for long-term monitoring of the average solar-neutrino flux and hence the mean solar luminosity over the last 4.31 millions years due to the long half-life $1.73(7) \times 10^7$ yr of ^{205}Pb [8]. Hence, such a measurement could shed light on the long-term stability of the Sun and therefore on the stability of stars in general [4].

First studies of the Tl experiment were done by [9–12] which later became the LOREX experiment (LORandite EXperiment) [13, 14]. While several experimental aspects have already been addressed or have been worked on, the major remaining uncertainty is the cross section for this reaction. Hence, it is essential to get a reliable estimate of this cross section and this work reports on calculation of this important quantity using current state-of-the-art techniques.

III. CALCULATION OF THE ^{205}Tl CROSS SECTION

The calculations for the neutrino-nucleus cross section are based on the Donnelly-Walecka method [15, 16] for

* joel.j.kostensalo@student.jyu.fi

† jouni.t.suhonen@jyu.fi

‡ zuber@physik.tu-dresden.de

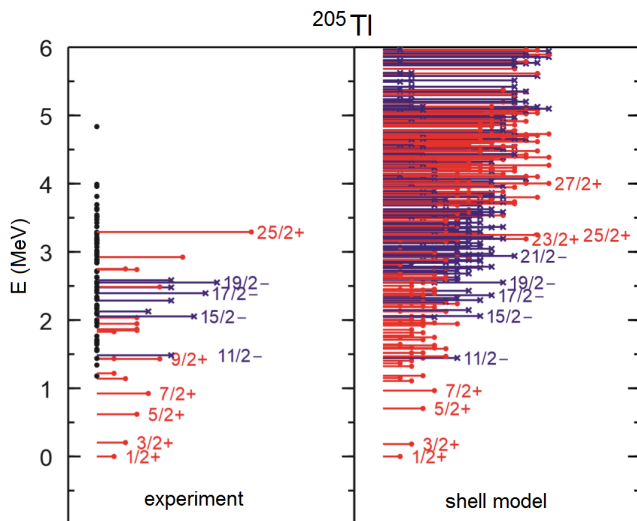


FIG. 1: Experimental and shell-model excitation spectra for ^{205}Tl . Each horizontal bar represents a nuclear state and its length is proportional to the angular momentum of the state.

the treatment of semi-leptonic processes in nuclei. Details of the formalism as it is applied here can be found from [17]. A streamlined version has also been given in the recent papers [18, 19].

The nuclear-structure calculations were done in the shell-model framework using the shell-model code NuShellX@MSU [20] with the Hamiltonian khhe [21] in the complete valence space spanned by the proton orbitals $0g_{7/2}$, $1d$, $2s$, and $0h_{11/2}$, and the neutron orbitals $0h_{9/2}$, $1f$, $2p$, and $0i_{13/2}$. As can be seen from Figures 1 and 2 the energy spectra of the relevant nuclei are reproduced astonishingly well. The half-life of ^{205}Pb is reproduced when $g_A = 0.75$ is adopted as the effective axial-vector coupling. This result is quite consistent with the previous calculations for beta decays in heavy nuclei [22]. In order to estimate the uncertainties related to nuclear structure, we consider here the range $g_A = 0.75$ – 1.00 for all transitions: a range which covers typical values adopted in large-scale shell-model calculations.

Since the exact energy of the low-lying states plays a significant role in determining the cross section for neutrinos with low energies, such as pp neutrinos, the energies of the dominating low-lying states were adjusted to their experimental values. The energy-adjusted states were the lowest two $1/2^-$ states and the lowest three $3/2^-$ and $1/2^+$ states. Based on the ordering of the levels in the shell-model calculation the state at 803 keV was taken to be $1/2^-$ and the state at 996 keV to be $3/2^-$.

The contributions by multipolarity are shown in Fig. 3 and by individual state in 4. The ground state of ^{205}Tl has the spin-parity $1/2^+$ so that Gamow-Teller type of transitions are possible only to $1/2^+$ and $3/2^+$ states in ^{205}Pb . There are only three known $1/2^+$ states in ^{205}Pb at 2795 keV, 4016 keV, and 4055 keV and no known $3/2^+$

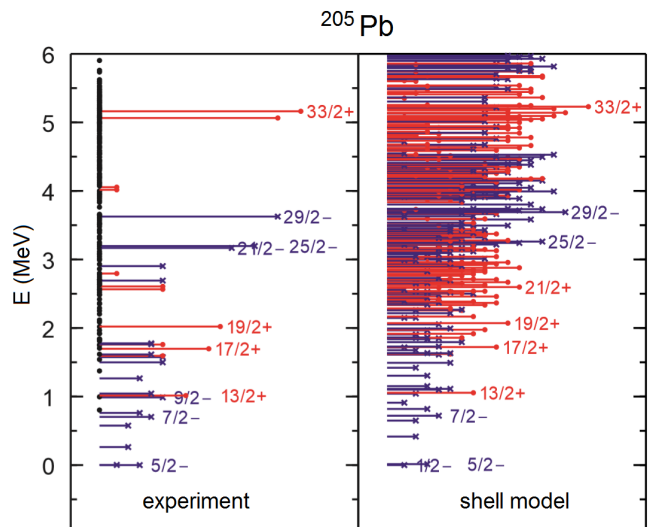


FIG. 2: Experimental and shell-model excitation spectra for ^{205}Pb . Each horizontal bar represents a nuclear state and its length is proportional to the angular momentum of the state.

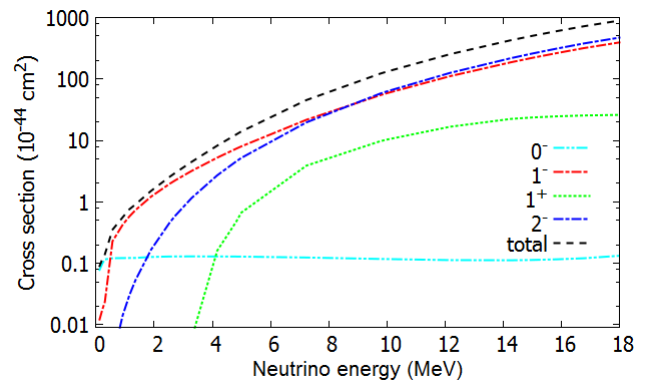


FIG. 3: Capture cross section for neutrino capture on ^{205}Tl as function of neutrino energy for the leading multiplicities with $g_A = 1.00$.

states. GT transitions are therefore available only for ^8B and hep neutrinos, which happen to have relatively low fluxes in the standard solar models [23]. For these higher-energy neutrinos the $1/2^+$ state at 4016 keV gives a noticeable contribution. Due to this lack of positive-parity states with small angular momenta, the cross section is dominated by spin-dipole type of forbidden transitions which render the total cross section smaller than expected from energy arguments alone.

IV. REACTION RATES IN SNU

Owing to the small cross section of low-energy neutrino-nucleus interactions, it is convenient to present the neutrino-capture rate in the solar-neutrino units

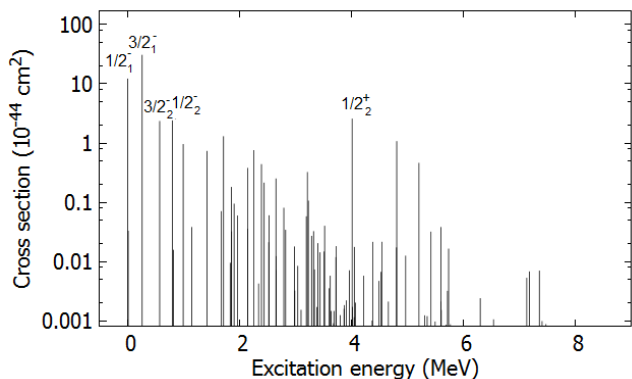


FIG. 4: Contributions of the individual states to the ${}^8\text{B}$ neutrino cross section with $g_A=1.00$. The horizontal axis gives the excitation energy in ${}^{205}\text{Pb}$.

(SNU), given as $1 \text{ SNU} = 10^{-36}$ capture reactions per target atom per second. Then the neutrino-capture rate R is described by

$$R = 10^{36} \sum_i \int \sigma(E) \phi_i(E) dE, \quad (3)$$

where $E, \sigma(E)$ and $\phi_i(E)$ are the neutrino energy, the neutrino-capture cross section (see the previous section) and the differential neutrino spectra. The latter are given at a distance of 1 astronomical unit (AU). The sum in (3) includes all 8 neutrino components from the pp and CNO cycle.

For the calculation of solar-neutrino capture rates the fluxes of the solar model BS05(OP) were adopted (see Table 2 in [23]) with the neutrino spectrum shapes avail-

able on John N. Bahcall's website [24]. With these spectra and fluxes we get for the capture rate 100.2 SNU with $g_A = 0.75$ and 132.4 SNU with $g_A = 1.00$ when the survival probability of electron neutrinos is not taken into account. With the electron-neutrino survival probability of 0.54 for the pp, ${}^7\text{Be}$, and ${}^{13}\text{N}$ neutrinos, and 0.50 for the pep, ${}^{15}\text{O}$, and ${}^{17}\text{F}$ neutrinos, and 0.36 for the ${}^8\text{B}$ neutrinos [25] we end up with a result of

$$R({}^{205}\text{Tl}) = 62.2 \pm 8.6 \text{ SNU} \quad (4)$$

for the capture rate.

V. SUMMARY AND CONCLUSIONS

Given the revived interest in solar-neutrino detection using ${}^{205}\text{Tl}$ due to its very small energy threshold we have performed a large-scale shell-model calculation to find out the cross section for the conversion of ${}^{205}\text{Tl}$ to ${}^{205}\text{Pb}$. Combined with the neutrino fluxes predicted by established solar models and taking into account the survival probabilities of electron neutrinos the capture rate turns out to be 62.2 ± 8.6 SNU. This capture rate is significantly smaller than anticipated by previous estimations.

VI. ACKNOWLEDGEMENT

The authors would like to thank Dr. Y. Litvinov to bring this issue to our attention. This work has been partially supported by the Academy of Finland under the Academy project no. 318043. J. K. acknowledges the financial support from Jenny and Antti Wihuri Foundation.

-
- [1] H. Ejiri, J. Suhonen, K. Zuber *Phys. Rep.* **797**, 1 (2019).
 - [2] G. M. Agostini et al., *Phys. Rev. D* **100**, 082004 (2018).
 - [3] B. T. Cleveland et al., *ApJ* **496**, 505 (1998).
 - [4] J. N. Bahcall, *Neutrino Astrophysics* (Cambridge Univ. Press, 1989).
 - [5] J. Kostensalo and J. Suhonen, *Phys. Lett. B* **781**, 480 (2018).
 - [6] J. Suhonen, *From Nucleons to Nucleus: Concepts of Microscopic Nuclear Theory* (Springer, Berlin, 2007).
 - [7] M. Wang et al. *CPC* **41**, 3 (2017).
 - [8] F. G. Kondev *NDS* **101**, 521 (2004).
 - [9] S. M. Freedman et al. *Science* **193**, 1117 (1976)
 - [10] S. M. Freedman et al. *Nucl. Instrum. Methods A* **271**, 267 (1988).
 - [11] P. Kienle *Nucl. Instrum. Methods A* **271**, 277 (1988).
 - [12] W. Henning and D. Schuell *Nucl. Instrum. Methods A* **271**, 324 (1988).
 - [13] M. K. Pavicevic *Nucl. Instrum. Methods A* **271**, 287 (1988).
 - [14] M. K. Pavicevic et al. *Adv. High Energy Phys.* **2012**, 274614 (2012).
 - [15] J. S. O'Connell, T. W. Donnelly, and J. D. Walecka, *Phys. Rev. C* **6**, 719 (1972).
 - [16] T. W. Donnelly and R. D. Peccei, *Phys. Rep.* **50**, 1 (1979).
 - [17] E. Ydrefors and J. Suhonen, *Adv. High Energy Phys.* **2012**, 373946 (2012).
 - [18] J. Kostensalo, J. Suhonen, and K. Zuber, *Phys. Rev. C* **97**, 034309 (2018).
 - [19] J. Kostensalo, J. Suhonen, C. Giunti, and P. C. Srivastava, *Phys. Lett. B* **795**, 542 (2019).
 - [20] B. A. Brown, W. D. M. Rae, *Nucl. Data Sheets* **120**, 115 (2014).
 - [21] E. K. Warburton and B. A. Brown, *Phys. Rev. C* **43**, 602 (1991).
 - [22] J. Suhonen, *Front. Phys.* **5**, 55 (2017).
 - [23] J. N. Bahcall et al., *Astrophys. J.* **621**, L85 (2005).
 - [24] J. N. Bahcall, Software and data for solar neutrino research, <http://www.sns.ias.edu/~jnb/> (cited 12/3/2019).
 - [25] M. Agostini et al. (The Borexino Collaboration), *Nature* **562**, 505 (2018).